Int. J. Electrochem. Sci., 7 **(2012)** 12236 - 12243

International Journal of
ELECTROCHEMICAL
SCIENCE
www.electrochemsci.org

Short Communication

Hydrothermal Synthesis of β-$Ni(OH)_2$ Nanoplates as Electrochemical Pseudocapacitor Materials

Yumei Ren[1,2], *Li Wang*[1,5], *Zhongjia Dai*[1], *Xiankun Huang*[1], *Jianjun Li*[1,5], *Ning Chen*[2], *Jian Gao*[1,5], *Hailei Zhao*[2], *Xiaoming Sun*[3], *Xiangming He*[1,4,*]

[1] Institute of Nuclear and New Energy Technology, Tsinghua University, Beijing 100084, PR China
[2] Department of Inorganic Nonmetallic Materials School of Material Science and Engineering, University of Science and Technology Beijing, Beijing, 100083, PR China
[3] State Key Laboratory of Chemical Resource Engineering, Beijing University of Chemical Technology, Beijing 100029, PR China
[4] State Key Laboratory of Automotive Safety and Energy, Tsinghua University, Beijing 100084, PR China
[5] Beijing Key Lab of Fine Ceramics, Tsinghua University, Beijing 100084, PR China
[*]E-mail: hexm@tsinghua.edu.cn

Received: 18 September 2012 / *Accepted:* 29 October 2012 / *Published:* 1 December 2012

β-$Ni(OH)_2$ nanoplates are synthesized by a hydrothermal process with sodium hydroxide as precipitator and nickel nitrate as nickel source. The effects are investigated with different reactant concentrations, reaction time, precipitators, pH values, and total concentrations. Phase structure and morphology of the samples are characterized by XRD and FESEM respectively. Supercapacitor performances are investigated using cyclic voltammetry (CV) and galvanostatic charge/discharge tests.

Keywords: $Ni(OH)_2$ Nanoplate; Hydrothermal; capacitor

1. INTRODUCTION

The development of efficient energy storage devices with high capacity and excellent stability is urgently needed to satisfy future social and environmental requirements [1-7]. Electrochemical capacitors (ECs), also known as supercapacitors or ultracapacitors, have caught much attention from researches to industry for their promise of delivering high level electrical powers and long operating lifetimes [8], so that they are also regarded as promising energy storage technologies [9]. A big limitation for using EC systems is their relatively low energy density compared with lithium batteries although they have superior power density and cycle life [10]. To improve the performances of

supercapacitors, many compounds have been investigated as the electrode materials, including carboneous materials, conducting polymers and transition-metal oxides/hydroxides [11]. Carboneous materials have relatively low specific capacitance, which is generally 100 to 300 F g^{-1}despite of their high charge/discharge cycling stability and high power densities [12]. Among transition-metal oxides, RuO_2 and IrO_2 exhibit excellent capacitive behaviors. And some conductive additive materials such as carbon nanotube and graphene have been used to improve the conductivity of the electrode materials [13]. However, high cost and environmental toxicity of Ru have limited it from practical applications [14]. Among transition-metal hydroxides, nickel hydroxide is an attractive candidate in supercapacitor applications due to its layered structure with large interlayer spacing, high theoretical specific capacitance and low cost [15].

Nickel hydroxide presents two polymorphs, α-$Ni(OH)_2$ and β-$Ni(OH)_2$. Although the alpha phase presents higher theoretical electrochemical capacity, it is a metastable turbostratic phase that rapidly changes to the beta phase during synthesis or in strong alkali media. Therefore, the beta phase is a better candidate as ECs material [16]. Modern electrochemical devices require the morphological control of the active material. The performance of $Ni(OH)_2$ is influenced by numerous factors, such as specific surface area, particle size, morphology, Faradic processes, etc[17]. β-$Ni(OH)_2$ nanoplates, synthesized by a hydrothermal process [18], have shown structure-dependent specific charge capacitances.

Hydrothermal process is a simple and promising method for material preparation, synthesized by which the products are uniform, highly pure, good dispersion, and have perfect morphologies [19]. In this study, β-$Ni(OH)_2$ nanoplates were synthesized by hydrothermal processes with nickel nitrate and sodium hydroxide as starting materials. This paves a simple way of time-saving and low cost to prepare high performance β-$Ni(OH)_2$.

2. EXPERIMENT

2.1 Material synthesis and Characterization

β-$Ni(OH)_2$ nanoplates were synthesized using $Ni(NO_3)_2{\cdot}6H_2O$(AR) and NaOH(AR) through a hydrothermal process. 0.0025 mol $Ni(NO_3)_2{\cdot}6H_2O$ was dissolved in 15 ml deionized water. The sodium hydroxide aqueous solution with the same concentration was prepared as mentioned above. The molar ratio of Ni^{2+}:OH^- was set as 1:1. The two types of aqueous solution were quickly mixed together, and then stirred for 15 minutes. The suspension was then sealed in 60 mL Teflon lined stainless steel autoclaves for hydrothermal reaction at 180 ℃ for 4 hours. The formed precipitates was collected by centrifuge, washed several times with distilled water and ethanol, and finally dried in oven at 80 ℃ in air. Pure β-$Ni(OH)_2$ was obtained by the aforementioned procedure, remembered as S sample.

The structure and phase analyses were performed using X-ray diffraction (XRD) with Cu $K_\alpha1$ and Cu $K_\alpha2$ radiation (Bruker D8 Advance X-ray diffractometer in a Bragg–Brentano configuration). The detected diffraction angle (2θ) was scanned from 10° to 80° with a scan speed of 0.01°s^{-1}[20]. Morphology and particle size were observed by field emission scanning electron microscope (FESEM, JEOL JSM-7001F).

2.2 Electrochemical measurement

78 wt% of the prepared active material, 20 wt% of acetylene black, and 2 wt% of polytetrafluoroethylene (PTFE) were mixed together in ethanol, and then ultrasonicated to ensure uniform mixing. The mixed slurry was drop-dried into a 1 cm ×1 cm Ni foam (2 mm thick) for 2 h at 70 ℃, compressed before measurement, and then dried again under vacuum at 140℃ for 12 h. All electrochemical measurements were carried out in a three-electrode compartment where a platinum plate was used as the counter electrode and a saturated calomel electrode (SCE) was used as the reference electrode. A 2M NaOH solution was used as the electrolyte. Electrochemical performances were evaluated by cyclic voltammetry (CV) and galvanostatic charge/discharge tests. Cyclic voltammetry scans were recorded from 0.0 V to 0.6 V at different scan rates. Galvanostatic charge/discharge tests were done from 0 to 0.4 V at different current densities. All electrochemical measurements were conducted on a CHI 660D electrochemical workstation (Shanghai CH Instrument Company, China).

3. RESULTS AND DISCUSSION

3.1 Material characterization

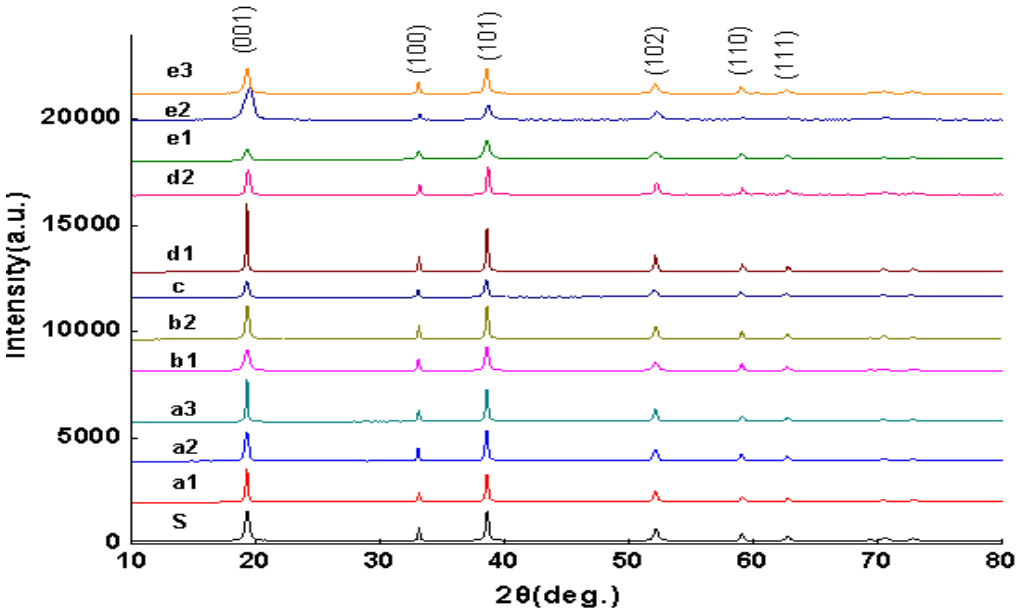

Figure 1. XRD patterns of β-Ni(OH)$_2$ nanoplates(nickel nitrate: Precipitator molar ratio: a1) 1:5, a2) 1:2, a3) 2:1; time:b1) 2h, b2) 8h; Precipitator: c) $NH_3 \cdot H_2O$; Reaction liquid concentration: d1) 2, d2) 0.5; pH: e1) 9, e2) 10, e3) 12)

Experimental conditions are summarized in Tab. 1 to discuss the effects of them on phase structures and morphologies of the samples clearly. Fig.1 shows XRD patterns of β-Ni(OH)$_2$ nanoplates at different experimental conditions. The results indicate that the Ni(OH)$_2$ patterns correspond to hexagonal phase β-Ni(OH)$_2$ [P-3m1(164), JCPDS Card No. 74-2075; a=3.13, c=4.63].

All of the diffraction lines are narrow and intensive, indicating that the sample is in a perfectly crystalline state[21]. No other peaks arising from impurities can be found, which means that β-$Ni(OH)_2$ crystals are successfully synthesized.

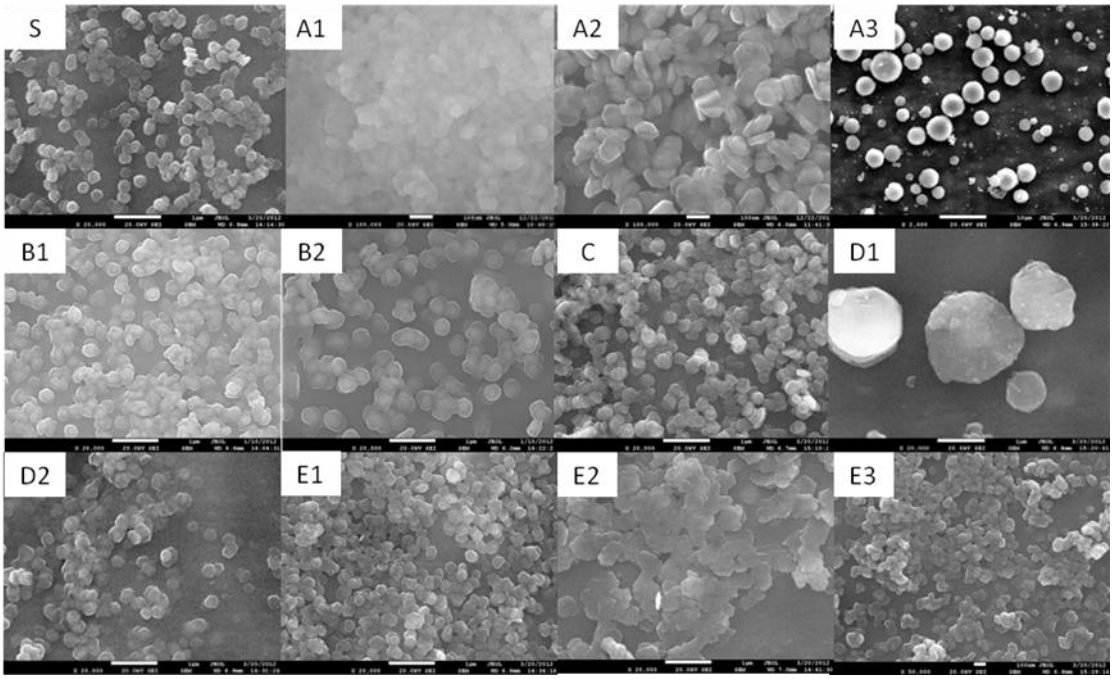

Figure 2. FESEM images of β-$Ni(OH)_2$ nanoplates (nickel nitrate: Precipitator molar ratio: A1) 1:5, A2) 1:2, A3) 2:1; time:B1) 2h, B2) 8h; Precipitator: C) $NH_3 \cdot H_2O$; Reaction liquid concentration: D1) 2, D2) 0.5; pH: E1) 9, E2) 10, E3) 12)

The surface morphologies of β-$Ni(OH)_2$ nanoplates are imaged by FESEM in Fig. 2, all samples are compared with sample S. It can be seen from A1, A2 and A3, with the decrease of molar ratio of Ni^{2+}: OH^-, the as-prepared nanoproducts are more regularly hexagonal flake and more uniform; the particle size is bigger; and the width-to-thickness ratio is larger. The amount of Ni^{2+} can control one-dimensional growth of products in a certain degree. However, the amount of Ni^{2+} is too much, which is beneficial to form close-grained microspheres instead of nanoflakes. As seen from B1 and B2, reaction time is two hours, the as-prepared nanoflakes are approximately hexagonal flake; while it's 4 hours, as-prepared products are regularly hexagonal flake; when it's as long as 8 hours, nanoplates appear adhesion between each other to some degree, and the reason may be Ostwald maturation. As shown in C, the target product is not obtained by a hydrothermal process with hexamethylenetetramine(HMT) as precipitator whose FESEM images are not shown; with ammonia water as precipitator, the obtained nanoplates are hexagonal flakes, and the particle distribution is common, but there is a little reunion phenomenon among flakes.

Table 1. Summary of experimental conditions, particle size and thickness of samples

Sample	nickel nitrate: Precipitator molar ratio	Time/h	Precipitator	Reaction liquid concentration	pH	Particle size/nm	Thickness /nm	XRD	SEM
S	1:1	4	NaOH	1	8	≈300	10-15	s	S
S1	1:5	4	NaOH	1	8	≈100	10-20	a1	A1
S2	1:2	4	NaOH	1	8	100-150	20-30	a2	A2
S3	2:1	4	NaOH	1	8	200-5000	-	a3	A3
S4	1:1	2	NaOH	1	8	≈300	20-30	b1	B1
S5	1:1	8	NaOH	1	8	≈300	20-30	b2	B2
S6	1:1	4	HMT	1	-	-	-	-	-
S7	1:1	4	$NH_3 \cdot H_2O$	1	8	≈300	20-30	c	C
S8	1:1	4	NaOH	2	8	800-2000	300	d1	D1
S9	1:1	4	NaOH	0.5	8	250-300	15-30	d2	D2
S10	1:1	4	NaOH	1	9	≈300	20-30	e1	E1
S11	1:1	4	NaOH	1	10	450-500	20-30	e2	E2
S12	1:1	4	NaOH	1	12	≈100	20-30	e3	E3

As indicated in D1 and D2, while reaction liquid concentration is doubled, it is interesting to observe that the $Ni(OH)_2$ nanoplates are stacked via their basal surfaces to form columnar structures with diameters ranging from 800 to 2000 nm and heights of 300 nm. The reason for this may be that pH of reaction liquid concentration is too large when it doubled. When initial pH value of reaction mixture is between 8 and 9, as shown by E1, E2 and E3, the products are regular hexagonal nanoplates with hexagonal structure, particle distribution is passable, and moreover, there is no obvious reunion phenomenon among nanoflakes. When initial PH value of reaction mixture is adjusted to 10, the nanoflakes are still hexagonal but not perfectly regular; the width-to-thickness ratio is larger than before; particle sizes of nanoflakes are not very unique; and also there are some irregular nanoparticles, which might be attributed to ultrasonic scanning in preparing SEM samples process[22]. The particle distribution is acceptable. When initial pH value of reaction mixture is adjusted to 12, the nanoflakes are still hexagonal but with smaller specific surface area, and there is obvious reunion phenomenon among nanoflakes, which may because of increasing initial pH value of reaction mixture.

3.2 Electrochemical characterization

Through discussing the effects of experimental conditions on β-$Ni(OH)_2$ nanoplates, it can be seen that as-obtained sample S11 nanoplates are regular hexagonal, largest width-to-thickness ratio, and good particle distribution.

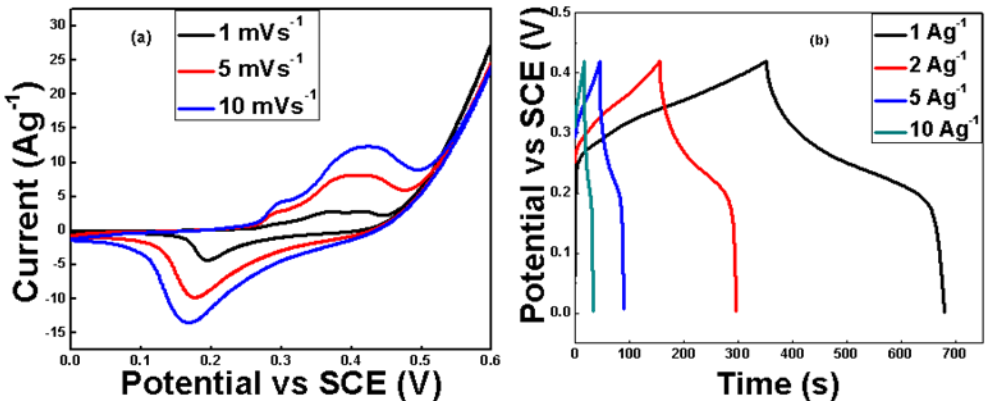

Figure 3. (a) Cyclic voltammograms and (b) galvanostatic charge/discharge curves of Sample 11

In order to discuss the influence of morphology of $Ni(OH)_2$ nanocrystals on capacitance performance, we evaluate the capacitance performance through anode current or cathode current of cyclic voltammetry curves. As shown in Fig 3 (a), with increase of scan rates, redox current increases, and redox peak gradually lags behind, but the cyclic voltammetry curves are still approximate symmetry, which indicates that the current has little influence on cyclic voltammetry curves. For the electrode of β-$Ni(OH)_2$ nanomaterials, oxidation process -$Ni(OH)_2$+OH^-↔$NiOOH+H_2O+e^-$occurs in the surface, restore process is the inverse process of the above electrode reaction. The active substances can finish relatively complete oxidation reaction at lower scan rate. The electrode shows reversible redox performance. However, at higher scan rate, the active substances have reached oxygen evolution potential before being completely oxidized. Electrode reaction is greatly affected by oxygen evolution reaction. The efficiency of the active material is low. Different charge/discharge curves close to a symmetric triangular, as shown in Fig 3 (b), indicating that the $Ni(OH)_2$ electrode shows pure capacitance properties. Specific capacitance could be calculated from the galvanostatic charge and discharge curves, using the following equation: $C=(It)/(mV)$, where I is charge or discharge current, t is the time for a full charge or discharge, m indicates the mass of the active material, and V represents the voltage change after a full charge of discharge. As shown in Tab 2, the specific capacitance of the sample is 793 F/g at a charge and discharge current density of 1A/g. With the increase of charge and discharge current, the specific capacitance gradually decreases. During large current charge/discharge process, active substances can't finish full redox. If we try with smaller charge and discharge current, the specific capacitance may be decreased less[23].

Table 2. Influence of current density on the specific capacitance at different current

Current(A/g)		1	2	5	10
specific capacitance (F/g)	pH=10	793	697	577	436

4. CONCLUSIONS

β-$Ni(OH)_2$ nanoplates can be synthesized by a hydrothermal process with sodium hydroxide as precipitator and nickel nitrate as nickel source. And when molar ratio of Ni^{2+}:OH^- is 1:1, reaction time is 4h, reaction temperature is 180℃, pH value of reaction mixture is 10, β-$Ni(OH)_2$ nanoplates are synthesized with regular hexagonal morphology, good dispersion, narrow particle size distribution range and large width-to-thickness ratio. Through electrochemical performance tests, β-$Ni(OH)_2$ shows a structure-dependence in their specific charge capacitances. The similar conclusions can be drawn with ammonia water as precipitator. These features are beneficial to make improvement of its performances and applications, which can also help to further improve electrochemical properties of electrode materials for lithium ion batteries.

ACKNOWLEDGEMENTS
This work is supported by the MOST (Grant No. 2011CB935902, No. 2010DFA72760, No. 2011CB711202 and No. 2013CB934000), the NSFC (Grand No.20901046 and No. 20903061), the Tsinghua University Initiative Scientific Research Program (Grand No. 2010THZ08116, No.2011THZ08139, No.2011THZ01004 and No. 2012THZ08129) and State Key Laboratory of Automotive Safety and Energy (grand No. ZZ2012-011).

References

1. L. Wang, X.M. He,W.T. Sun, J.W. Guo, J.J. Li, J. Gao, C.Y. Jiang, *Angew. Chem. Int. Ed.*, 51(2012) 9034–9037
2. L. Wang, N. Li, X.M. He, C.R. Wan, C.Y. Jiang, J. Electrochem. Soc., 159(2012) A915-A919.
3. L. Wang, X.M. He, J.W. Guo, J.J. Li, J. Gao, C.Y. Jiang, C.R. Wan, J. Mater. Chem., 22(2012) 22077-22081.
4. L. Wang, X.M. He, J.J. Li, M. Chen, J. Gao, C.Y. Jiang, *Electrochimica Acta*, 72(2012) 114-119.
5. L. Wang, W.T Sun, X.M. He, J.J. Li, J. Gao, C.Y. Jiang, *Int. J. Electrochem. Sci.*,7(2012) 3591-3600
6. L. Wang, L.W. Zhang, X.M. He, J.J. Li, J. Gao, C.Y. Jiang, *Int. J. Electrochem. Sci.*,7(2012) 3362-3370**.**
7. J.W. Zhu, S. Chen, H. Zhou, X. Wang, *Nano Res*. 5 (1) (2012) 11-19.
8. P. Lu, D.F. Xue, H. Yang, Y.N. Liu, *Int. J. S. Nano. Mater*. 2012 1-25.
9. K. Naoi and P. Simon, *Electrochem. Soc. Interface Spring*, , 17(2008)34-37
10. Z. Tang, C.H. Tang, H. Gong, *Adv. Funct. Mater*. 22 (2012) 1272-1278.
11. H.Y. Wu, H.W. Wang, *Int. J. Electrochem. Sci*. 7 (2012) 4405-4417.
12. Z.P. Sun, X.M. Lu, Ind. Eng. Chem. Res. 2012, dx.doi.org/10.1021/ie202706h, in press.
13. S. Xing, Q. Wang, Z.C. Ma, Y.S. Wu, Y.Z. Gao, *Mater. Lett*. 78 (2012) 99-101.
14. J.P. Liu, C.W. Cheng, W.W. Zhou, H.X. Li, H.J. Fan, *Chem. Commun*. 47 (2011) 3436-3438.
15. S.B. Yang, X.L. Wu, C.L. Chen, *Chem. Commun*. 48 (2012) 2773-2775.
16. S. Cabanas-Polo, K.S. Suslick, A.J. Sanchez-Herencia, *Ultrason. Sono- chem*. 18 (2011) 901-906.
17. J. Jiang, J.P. Liu, R.M. Ding. *ACS Appl. Mater. Interfaces*, 3 (2011) 99-103.
18. X.J. Zhang, W.H. Shi, J.X. Zhu, *Nano Res*. 3 (9) (2010) 643-652.
19. X.M. Fu, H. Sun, X.F. Wang, Z.W. Zhao, *Inorg. Chem. Ind.* 43 (11) 2011 34-36.
20. G. P. Wang, L. Zhang, J. Kim, J.J. Zhang, *J. Power Sources* 2011, *J. Power Sources* 217(2012) 554–561.

21. J.Q. Liu, J.L. Shi, X. Yan, X.L. Zhai, Z.C. Tao, Q.U. Guo, L. Liu, *Int. J. Electrochem. Sci.*,7(2012) 2214-2220
22. G.R. Fu, Z.A. Hu, L.J. Xie, X.Q. Jin, Y.L. Xie, Y.X. Wang, Z.Y. Zhang, Y.Y. Yang, H.Y. Wu, *Int. J. Electrochem. Sci.*,4(2009) 1052-1062
23. H.Y. Wu, H.W. Wang, *Int. J. Electrochem. Sci.*,7(2012) 4405-4417.